*Quantum Electronics* **34** (3) 255 – 260 (2004) 

*LASER BEAMS*

PACS numbers: 42.25.Bs; 42.30.Va; 42.60.Jf
DOI: 10.1070/QE2004v034n03ABEH002623

# On a method for obtaining laser beams with a phase singularity

A.A. Malyutin

***Abstract*. A method is analysed for obtaining laser beams with a phase singularity with the help of phase screens described by the function of the type $\exp(il\varphi)$. It is shown that this method is used to obtain laser beams in the form of single rings with a smooth intensity distribution in the far-field radiation zone (at the lens focus) representing the superposition of Laguerre – Gaussian modes. In the near-field zone and, in the presence of aperture clipping, also in the focal region, the beams with a more complicated structure can be observed. The scaling of the radius corresponding to the maximum intensity of the beam both in the absence and presence of aperture clipping occurs linearly with the singularity charge *l*. The influence of the beam decentration and of the phase screen on the structure of phase-singularity beams is estimated.**

***Keywords***: *laser beams, phase singularity, mode composition of radiation.*

## 1. Introduction

Light beams with phase singularities [phase-singularity beams (PSBs)], which are also called 'optical vortices' due to the specific wave-front structure, have been extensively studied in the last decade. These beams attract interest because they can be used to manipulate micron and submicron objects in biology, microelectromechanics, microhydrodynamics, etc. Due to specific properties of their propagation in linear and nonlinear media, PSBs are also of interest from the theoretical point of view.

At present PSBs are obtained, as a rule, using either the transformation of the Hermite – Gaussian (HG) modes $u_{nm}^{\mathrm{HG}}$ (commonly with $n = 0$ and $m > 0$) by means of astigmatic $\pi/2$ converters [1] or synthesised computer holograms [2]. In the first case, pure Laguerre – Gaussian (LG) modes $u_{pl}^{\mathrm{LG}}$ [$p = \min(n, m)$, $l = n - m$] are obtained under certain conditions. However, it is rather difficult to match the input-beam parameters with the optical parameters of the $\pi/2$ converter. An example is paper [3] (see Fig. 4 in it) where insufficient matching between these parameters resulted in a change in the beam scale after the converter rotation (this was explained in our paper [4]). As a result, the output radiation of the converter consists generally of a set of LG modes [5]. In a particular case, it is possible to obtain elliptic LG modes [4], which are convenient, for example, for manipulations with elongated microobjects. The elliptic LG modes, which possess astigmatism, can exist only in a limited spatial region and are, naturally, also a superposition of pure LG modes.

When computer holograms are used, which are in fact the interference pattern of the PSB and one or another reference beam ($\mathrm{TEM}_{00}$ modes with the spherical [2] or inclined [6] wave front), along with the required radiation, also radiation in extra diffraction orders is obtained, which should be filtered. This can substantially reduce the conversion efficiency.

Recently, a method for obtaining PSBs was used in several papers [7 – 11], which is similar to the holographic method, where a singularity of the type $\exp(il\varphi)$ is introduced to the laser beam directly by means of a phase screen (kinoform). A great number of elements ($480 \times 480$) of a controlled liquid-crystal phase screen used in the method made it possible to obtain beams with the topological singularity charge $l$ up to 200 [10]. The efficiency of this method, according to Ref. [9], can approach 100 %.

In this paper, we analyse the structure and mode composition of PSBs obtained with the help of phase screens, which are described by a function of the type $\exp(il\varphi)$. We consider the near- and far-field radiation zones and the influence of the form of the initial laser beam and its position with respect to the phase-screen axis on the field pattern.

## 2. $\mathrm{TEM}_{00}$ mode and a phase screen with $\Phi = \exp(il\varphi)$

### 2.1 Far-field radiation zone

Consider the $\mathrm{TEM}_{00}$ radiation mode with the unit intensity, the radius $w$, and the plane wave front propagating through a phase screen, whose phase $\Phi$ depends on the azimuthal angle $\varphi$ as $\Phi = \exp(il\varphi)$, where $l$ is an integer (the singularity charge). Then, the radiation field at the transparency output can be written in the form

$$u(\rho, \varphi) = \exp\left(-\rho^2/w^2 + il\varphi\right). \quad (1)$$

We assume that this radiation is focused by a lens with the focal distance $f = \pi w^2/\lambda$, as shown in Fig. 1.

**A.A. Malyutin** A.M. Prokhorov General Physics Institute, Russian Academy of Sciences, ul. Vavilova 38, 119991 Moscow, Russia; tel.: (095) 135-03-27; fax: (095) 135-20-55; e-mail: amal@kapella.gpi.ru

Received 3 July 2003
*Kvantovaya Elektronika* **34** (3) 255 – 260 (2004)
Translated by M.N. Sapozhnikov

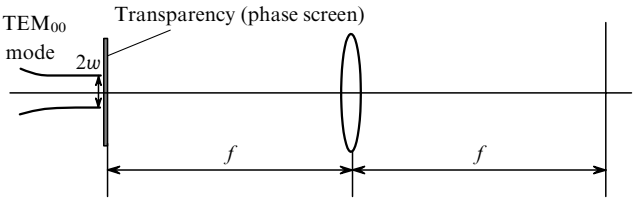


**Figure 1.** Optical scheme for obtaining phase-singularity beams using a phase screen with $\Phi = \exp(il\varphi)$.

The field distribution in the lens focus is described by the Fourier transform of field (1). This distribution can be written in cylindrical coordinates, by making the substitution $r \to r/(\lambda f)$:

$$U(r,\theta) = \frac{1}{2\pi}\int_{-\pi}^{+\pi}\int_{0}^{\infty} u(\rho,\varphi)\exp[-i2\pi r\rho\cos(\theta-\varphi)]\rho d\rho d\varphi. \quad (2)$$

By using expressions (2.5.41.10) from Ref. [12] and (6.631.7) from Ref. [13], we obtain

$$U(r,\theta) = Brw\exp\left[il(\theta-\pi/2)-\gamma r^2\right] \times\left[I_{(l-1)/2}(\gamma r^2) - I_{(l+1)/2}(\gamma r^2)\right], \quad (3)$$

where $B$ is a constant; $I_\nu(z)$ is the modified Bessel function of the imaginary argument; and $\gamma = 1/(2w^2)$. Because a sequence of the integer and half-integer indices of the Bessel function corresponds to the series $l = 1, 2, 3, ...$, we can perform the transformations in the right-hand side of (3):

$$I_0(\gamma r^2) - I_1(\gamma r^2) = \sum_{k=0}^{\infty}\frac{(\gamma r^2/2)^{2k}(k+1-\gamma r^2/2)}{k!(k+1)!} \quad (4)$$

for $l = 1$ and

$$I_{1/2}(\gamma r^2) - I_{3/2}(\gamma r^2) = \frac{1}{r}\left(\frac{2}{\pi\gamma}\right)^{1/2}\left[\sinh(\gamma r^2) - \cosh(\gamma r^2) + \frac{\sinh(\gamma r^2)}{\gamma r^2}\right] \quad (5)$$

for $l = 2$, etc.

Therefore, for odd values of $l$, the field is represented as sums, while for even values of $l$, the field is represented by hyperbolic secant and cosecant. The far-field radiation distributions in the absence of diffraction due to aperture restrictions have the form of a single ring independent of the parity of $l$ and are quite similar to each other (Fig. 2).

To find the dependence of the position of the maximum of distribution (3) on $l$, it is convenient take, for example, $l = 2n + 1$. Then, the equation $dU/dr = 0$ is reduced to the equation

$$\left(\frac{2n+1}{\gamma r_{\max}^2} - 4\right)I_n(\gamma r_{\max}^2) + \left(\frac{2n+1}{\gamma r_{\max}^2} + 4\right)I_{n+1}(\gamma r_{\max}^2) = 0. \quad (6)$$

The numerical solution of (6) for odd $l$ gives

$$r_{\max} \approx [0.595 + 0.662(l-1)/2]/\sqrt{\gamma}. \quad (7)$$

The FWHM of the ring increases also approximately linearly with $l$.

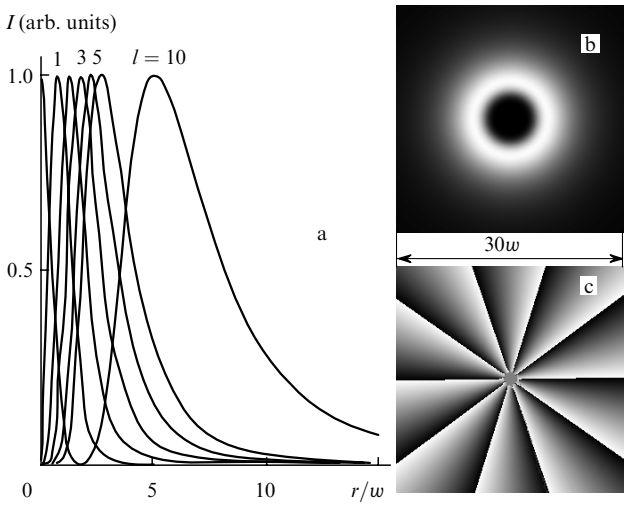


**Figure 2.** Dependences of the intensity of field (3) on the radial coordinate (curves are normalised to their maxima) (a) and the distributions of the intensity (b) and phase (c) in the PSB for $l = 10$ (the phase change from 0 to $2\pi$ is given on a linear 'grey' scale).

The difference in the use of phase screens with odd and even $l$ cannot seemingly have a physical meaning, and the difference between (4) and (5) is purely symbolic. However, actually this is not the case: when the same basis of the LG mode is used, the fields produced by means of phase screens with different singularity charges have different ratios of the real and imaginary parts of the expansion coefficients (mode amplitudes) $A_{pl} = a_{pl} + ib_{pl}$. Figure 3 shows the numerical expansions of fields (4) and (5) in the LG modes. For $l = 1$, we have

$$U(r,\theta,l=1) \approx \sum_{p=1}^{\infty}(a_{p1} + ib_{p1})u_{p1}^{LG} \quad (8)$$

and the spectrum contains the $u_{p1}^{LG}$ modes (Fig. 3a), for which $a_{p1} \neq 0$ and $b_{p1} \neq 0$. Equality (8) is approximate due to the presence of the error in the expansion. The error value can be estimated from the fact that the orthogonality condition for the LG modes in the calculation is fulfilled with the accuracy $\sim 10^{-8}$–$10^{-7}$. According to this calculation, we have $|a_{p1}| = |b_{p1}|$ with the above accuracy. For $l = 2$, we have

$$U(r,\theta,l=2) \approx \sum_{p=0}^{\infty}(a_{p2} + ib_{p2})u_{p2}^{LG} \quad (9)$$

and, as one can see from Fig. 3b, the mode amplitudes in the spectrum are either real or imaginary. The amplitude moduli for expansions (8) and (9) as functions of $p$ are shown in Figs 3c, d. Note that a passage to another basis of modes $u_{pl}^{LG}$ (for example, the basis rotation by multiplying each of the modes by a constant factor $\exp(i\psi)$, where $\psi$ is a constant) will result in the corresponding rotation of spirals in Figs 3a, b. In this case, naturally, the distributions of the amplitude moduli (Figs 3c, d) will not change.

Similar properties are also observed for other even and odd values of $l$ for the phase screen. As $l$ increases, the weight of the LG modes with higher radial indices $p$ in the expansion also increases. This is already noticeable in Figs 3c, d on passing from $l = 1$ to $l = 2$.

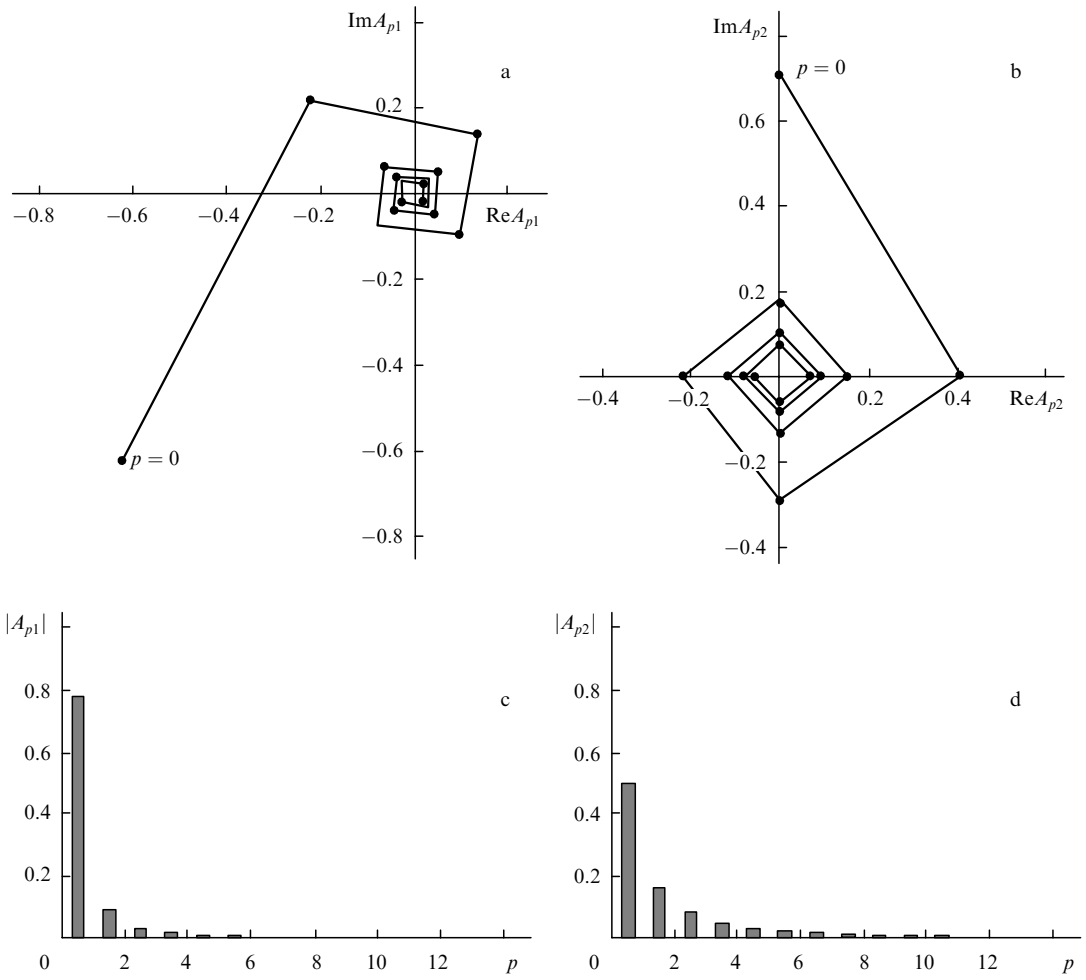


**Figure 3.** Amplitudes in the expansions of field (3) in the LG modes (a, b) and dependences of the moduli of these amplitudes on the index $p$ (c, d) for a phase screen with $l = 1$(a, c) and 2 (b, d). The points on spirals correspond to $p = 0, 1, 2, \ldots$ .

### 2.2 Near-field radiation zone

According to Ref. [14], the Fourier transform of the HG function for any integer or fractional (including irrational [15]) order $a$ is

$$\mathscr{F}^{a}\left[\exp(-\pi x^2)H_n(x\sqrt{2\pi})\right] = \exp(-\mathrm{i}an\pi/2)\exp(-\pi\xi^2)H_n(\xi\sqrt{2\pi}). \quad (10)$$

By expanding the LG modes in the HG modes [1]

$$u_{pl}^{\mathrm{LG}}(x,y,z) = \sum_{k=0}^{N} \mathrm{i}^k b(n,m,k) u_{N-k,k}^{\mathrm{HG}}(x,y,z) \quad (11)$$

expression (10) can be written in the form

$$\mathscr{F}^{a}\left[u_{pl}^{\mathrm{LG}}(x,y,z)\right] = \exp(-\mathrm{i}aN\pi/2)u_{pl}^{\mathrm{LG}}(x,y,z), \quad (12)$$

where $N = n + m = 2p + |l|$ is the mode order. In our case, $\mathscr{F}^{a} = \mathscr{F}^{1}$ and the inverse Fourier transform of field (3), taking into account the accumulation of the Gouy phase during the propagation of the beam to the focal plane of a lens with the focal distance $f$ (Fig. 1), has the form

$$\mathscr{F}^{-1}[U(r,\theta,l)] = \sum_{p=0}^{\infty} A_{pl}\exp[\mathrm{i}(2p + |l| + 1)\pi/2]u_{pl}^{\mathrm{LG}} = u(\rho,\varphi). \quad (13)$$

The mode composition of radiation (3) in the far-field zone is inherent in the input plane in Fig. 1 and in all intermediate points at the optical axis. In the latter case, we obtain the expression

$$A_{pl}(z) = [a_{pl}(z=0) + \mathrm{i}b_{pl}(z=0)] \times \exp[-\mathrm{i}(2p + |l| + 1)\psi(z)], \quad (14)$$

for the expansion coefficients of initial field (1), where $\psi(z) = \arctan(z/z_{\mathrm{R}})$ is the Gouy phase and $z_{\mathrm{R}} = \pi w^2/\lambda$ is the Rayleigh length of the beam (beam waist length). Therefore, the expansion coefficients for different $z$ differ only in phase additions corresponding to the LG mode indices.

These coefficients for initial field (1) and its far-field zone are determined by relation (13). For $l = 1$, the exponential term in (13) is reduced to $(-1)^{2(p+1)}$, and for $l = 2$, to $\mathrm{i}^{2p+1}$. Therefore, in the first case, the spiral in Fig. 3a is rotated through 180° (see Fig. 4a) and in the second case, the spiral in Fig. 3b is rotated through 90° (see Fig. 4b). At points $z$ between the phase screen and the focal plane of the lens, each of the complex coefficients $A_{pl}$ (14) of the basis LG modes rotates in accordance with a change in the Gouy phase. This is shown for some values of $z$ for $l = 2$ in Figs 4c, d. Due to the dependence of the angle of rotation

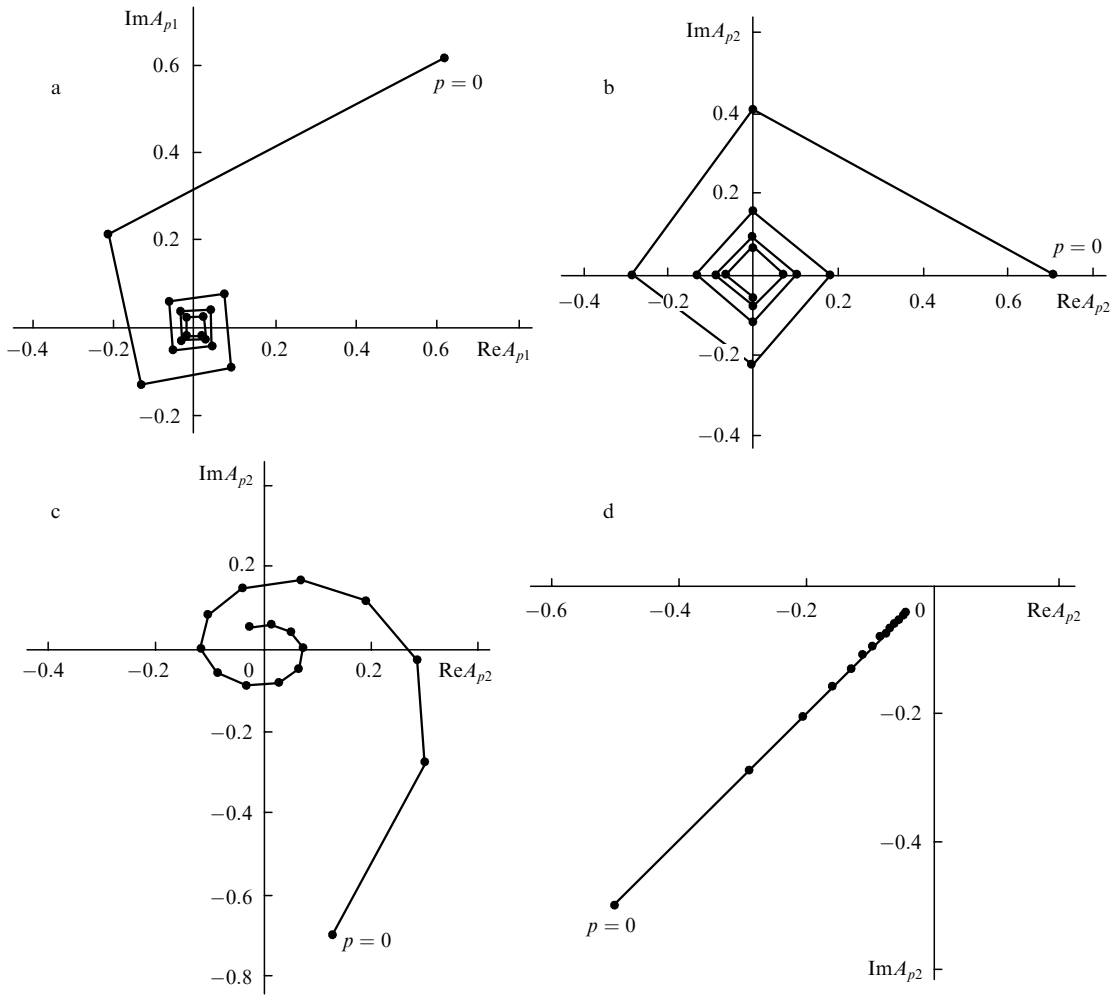


**Figure 4.** Amplitudes in the expansions of field (1) in the LG modes in the plane of a phase screen with $l = 1$ (a) and 2 (b) and changes of these amplitudes for $l = 2$ upon the propagation of the beam by the distance $z = z_R/2$ (c) and $z_R$ (d). The points on spirals correspond to $p = 0, 1, 2, \ldots$.

on $p$, the radius vectors of the inner points of the spiral in Fig. 3a rotate through the angle proportional to $p$ (Fig. 4c), and for $z = f = z_R$, the spiral transforms to a straight line (Fig. 4d). As the beam further propagates toward the focal plane of the lens, the spiral is twisted, but already in the opposite direction. It transforms from the spiral twisted counter-clockwise at the point $z = 0$ (Fig. 4b) to a similar spiral twisted clockwise at the point $z = 2f = 2z_R$ (Fig. 3b).

The near-field radiation distribution is intermediate between fields (1) and (3) in accordance with the change in the coefficients of expansion in LG modes (14). These fields, as follows from the numerical simulation of the PSB propagation (Fig. 5) are not monotonically smooth. Note that the maximum intensity of the field at a distance of $0.01z_R$ behind the phase screen ($l = 10$) exceeds the intensity of the initial $TEM_{00}$ mode by a factor of 2.25. At the same time, the field intensity at the focus of a lens with $f = z_R$ proves to be much lower (0.0054 of the initial intensity).

### 2.3 Effects of diffraction and decentration

The authors of paper [10] analysed the structure of the $TEM_{00}$ mode behind a screen with $\Phi = \exp(il\varphi)$ and explained the linear dependence of the position of the maximum intensity of the PSB by the influence of diffraction from the aperture of a focusing lens. They repeated this conclusion in paper [16]. As shown above, linear dependence (7) is an inherent feature of the beam obtained by means of a phase screen with $\Phi = \exp(il\varphi)$.

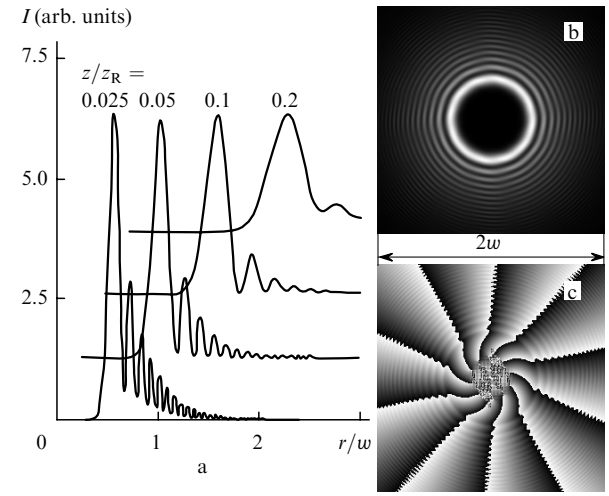


**Figure 5.** Radial distributions of the field intensity behind the phase screen ($l = 10$) in the near-field zone (the relative intensities of the curves are not met) (a) and the distributions of the PSB intensity (b) and phase (c) at a distance of $0.01z_R$ from the phase screen (the intensity maximum amount to 225 % of the initial beam intensity).

However, it is rather difficult to avoid aperture effects, at least upon focusing by objectives with a very short focal distance and a very large numerical aperture (achieved mainly due to immersion). The matter is that the phase screen represents a matrix device based on liquid crystals [8, 10]. The full size of the matrix is $2 \times 2$ cm, which makes the use of the initial $TEM_{00}$ beam with a rather large cross section optimal. It seems impossible to avoid vignetting in matching this beam with a relatively small input pupil of a short-focus microobjective. This explains the field structure consisting of many rings observed in the focal plane [10, 16] instead of one ring, as should be in the absence of aperture clipping (see section 2.1).

The numerical simulation, which was performed, as above, using the FRESNEL program [17], showed that, when the intensity of the initial $TEM_{00}$ beam was clipped at the 5 % level of the maximum intensity ($\sim 22.4$ % in the field) and the multiring structure was observed at the lens focus (Fig. 6a), the maximum intensity even increased compared to the intensity of the distribution in Fig. 2b. The replacement of the $TEM_{00}$ mode at the phase-screen input by a beam with a flat top, the same radius $w$ and intensity leads to a further increase in the maximum intensity of the PSB. In this case, the clipping of a Gaussian beam or passing to a flat-top beam is accompanied by a shift of the intensity maximum to the region of larger values of $r/w$ (Fig. 6b).

The PSB quality also depends on the decentration between the initial beam and the phase screen. Due to the vector nature of the orbital moment imparted to the beam, the displacement of the centre of the initial beam (for example, along the $x$ axis) corresponds to the displacement of the 'centre of gravity' of the PSB and the deformation of its intensity distribution along the $y$ axis (Figs 6c, d). The dependence of the position of the 'centroid' in the far-field zone on $l$, according to the results of the numerical experiment for a Gaussian beam (Fig. 6c), can be written in the form

$$\boldsymbol{r}_c = \frac{\lambda F}{\pi w^2}\boldsymbol{l} \times \boldsymbol{r}_b, \tag{15}$$

where $\boldsymbol{r}_c$ and $\boldsymbol{r}_b$ are the radius vectors of the 'centroid' of the PSB and the centre of a Gaussian beam, respectively, with respect to the phase-screen axis. The coefficient in front of the vector product characterises a change in $\boldsymbol{r}_c$ when the focal distance $F$ of the lens differs from $f = z_R$ (Fig. 1). Note that the fixed displacement $\boldsymbol{r}_b$ corresponds to a constant, independent of $l$, ratio of the maxima in the left and right parts of the PSB intensity distributions in Fig. 6d.

## 3. Conclusions

It is shown that PSBs generated using the $TEM_{00}$ mode and a phase screen (kinoform) with $\Phi = \exp(il\varphi)$ in the absence of diffraction represent a superposition of the LG mode with a fixed value of $l$, which is 'continuous' over the radial index $p$. The far-field intensity distribution of these beams

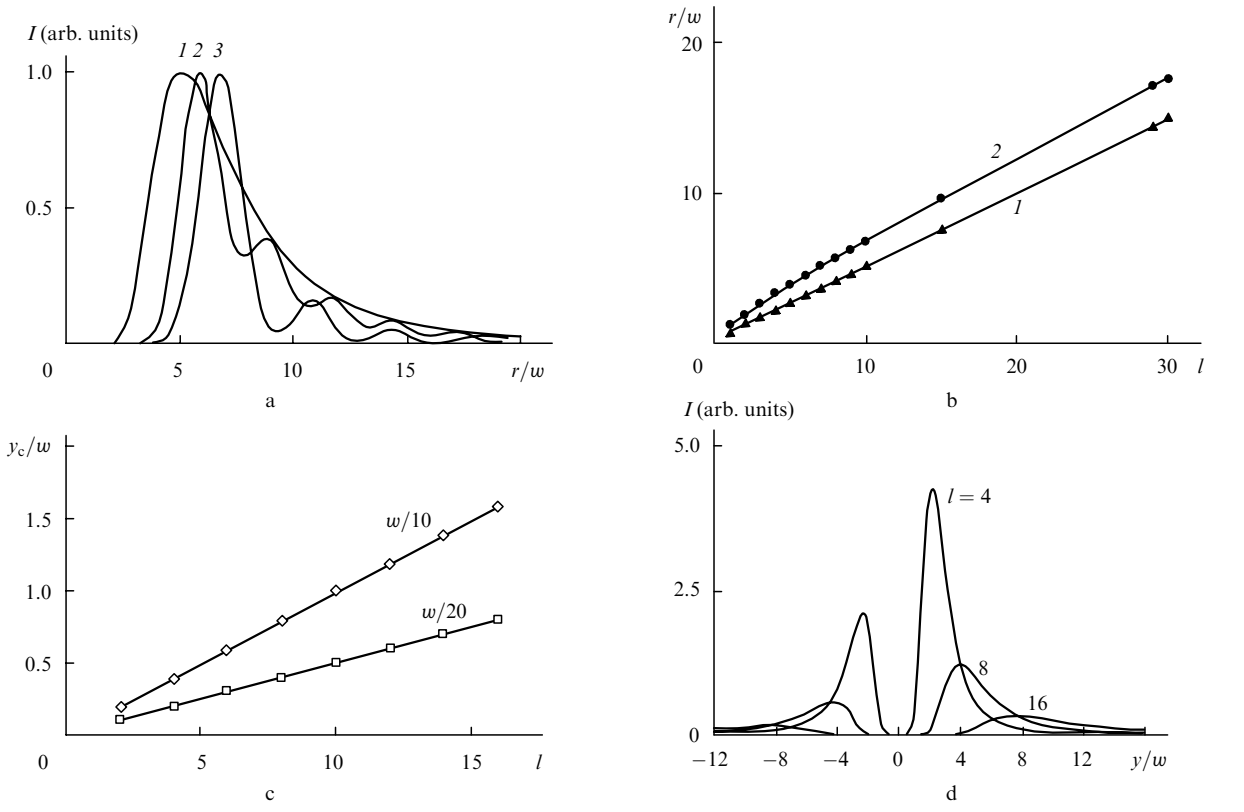


**Figure 6.** (a) Radial distributions of the field intensity behind the phase screen ($l = 10$) in the far-field zone (the relative intensities of the curves are not met) for the Gaussian beam at the input (*1*), the clipped (at the 5 % level) Gaussian beam (*2*), and the flat-top beam (radius $w$) (*3*); (b) dependences of the position of the maximum intensity on the singularity charge $l$ for the Gaussian beam (*1*) and the flat-top beam (*2*); changes in the position of the 'centroid' of the PSB (along the $y$ axis) upon displacements of the Gaussian beam $\Delta x = w/10$ and $w/20$ and different $l$ (c) and deformations of the PSB intensity distribution along the $y$ axis ($\Delta x = w/10$) (d).

has the form of single rings with the radial position of the intensity maximum and half-width proportional (with a rather high accuracy) to the singularity charge $l$. The linear dependence on $l$ is retained in the presence of aperture clipping and when a flat-top beam is used instead of the initial $TEM_{00}$ beam. In the near-field zone, and in the case of diffraction, also in the far-field zone, PSBs have the multiring structure. The PSB structure also depends substantially on the decentration of the initial Gaussian beam with respect to the phase screen, at which the displacement of the 'centroid' of the PSB is proportional to the vector product $\boldsymbol{l} \times \boldsymbol{r}$.

***Acknowledgements.*** This work was supported by the Russian Foundation for Basic Research (Grant No. 02-02-17718).

## References

1. Beijersbergen M.W., Allen L., van der Veen H.E.L.O., Woerdman J.P. *Opt. Commun.*, **96**, 123 (1993).
2. Heckenberg N.R., McDuff R., Smith C.P., White A.G. *Opt. Lett.*, **17**, 221 (1992).
3. O'Neil A.T., Courtial J. *Opt. Commun.*, **181**, 35 (2000).
4. Malyutin A.A. *Kvantovaya Elektron.*, **33**, 235 (2003) [*Quantum Electron.*, **33**, 235 (2003)].
5. Courtial J., Padgett M.J. *Opt. Commun.*, **159**, 13 (1999).
6. Heckenberg N.R., McDuff R., Smith C.P., Rubinsztein-Dunlop H., Wegener M.J. *Opt. Quantum Electron.*, **24**, S951 (1992).
7. Beijersbergen M.W., Coerwinkel R.P.C., Kristensen M., Woerdman J.P. *Opt. Commun.*, **112**, 321 (1994).
8. Curtis J.E., Koss B.A., Grier D.G. *Opt. Commun.*, **207**, 169 (2002).
9. Ganic D., Gan X., Gu M., Hain M., Somalingam S., Stankovic S., Tschudi T. *Opt. Lett.*, **27**, 1351 (2002).
10. Curtis J., Grier D.G. *Phys. Rev. Lett.*, **90**, 133901 (2003).
11. Zhang D.W., Yuan X.-C. *Opt. Lett.*, **28**, 740 (2003).
12. Prudnikov A.P., Brychkov Yu.A., Marichev O.I. *Integraly i ryady* (Integrals and Series) (Moscow: Nauka, 1981).
13. Gradshtein I.S., Ryzhik I.M. *Tablitsy integralov, summ, ryadov i proizvedenii* (Tables of Integrals, Sums, and Products) (Moscow: Fizmatgiz, 1963).
14. Bultheel A., Martinez H. *A Shattered Survey of the Fractional Fourier Transform* (Katholieke Universiteit Leuven, Report TW337, 2002).
15. James D.F.V., Agarwal G.S. *Opt. Commun.*, **126**, 207 (1996).
16. Curtis J.E., Grier D.G. *Opt. Lett.*, **23**, 872 (2003).
17. Epatko I.V., Malyutin A.A., Serov R.V., Solov'ev D.A., Chulkin A.D. *Kvantovaya Elektron.*, **25**, 717 (1998) [*Quantum Electron.*, **28**, 697 (1998)].